Supporting Information for

# Manipulating Interfacial Stability *via* Absorption-Competition Mechanism for Long-Lifespan Zn Anode

Meijia Qiu[1, 2], Liang Ma[2], Peng Sun[1, 2], Zilong Wang[2], Guofeng Cui[1, *], Wenjie Mai[2]

[1]Key Laboratory for Polymeric Composite & Functional Materials of Ministry of Education, School of Chemistry, Key Laboratory of Low-carbon Chemistry & Energy Conservation of Guangdong Province, Sun Yat-sen University, Guangzhou 510275, People's Republic of China

[2]Siyuan Laboratory, Guangdong Provincial Engineering Technology Research Center of Vacuum Coating Technologies and New Energy Materials, Guangzhou Key Laboratory of Vacuum Coating Technologies and New Energy Materials, Department of Physics, Jinan University, Guangdong 510632, People's Republic of China

*Corresponding author. E-mail: cuigf@mail.sysu.edu.cn (Guofeng Cui)

## Supplementary Figures

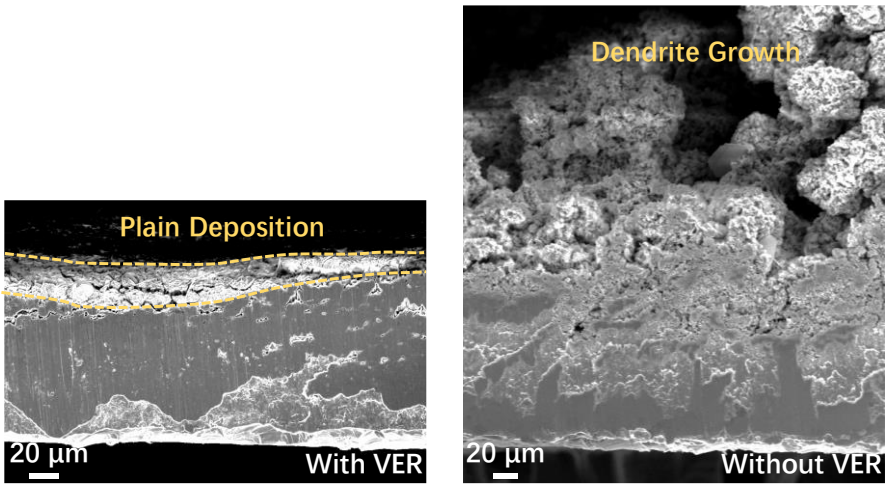


**Fig. S1** Cross-sectional SEM images of Zn sheet surface with (left) and without (right) the veratraldehyde additive

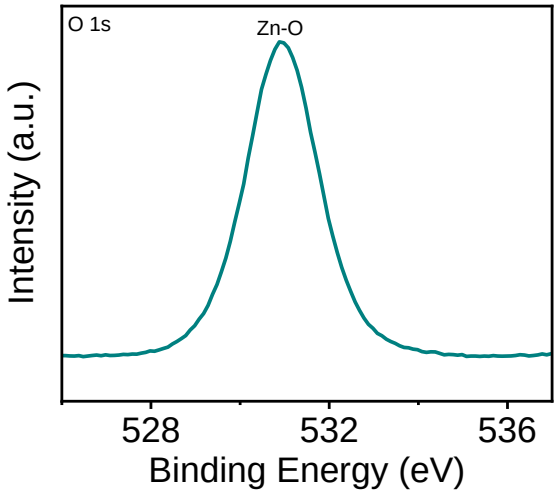


**Fig. S2** The high-resolution XPS spectra of O 1s for the Zn sheet after soaked in DI water

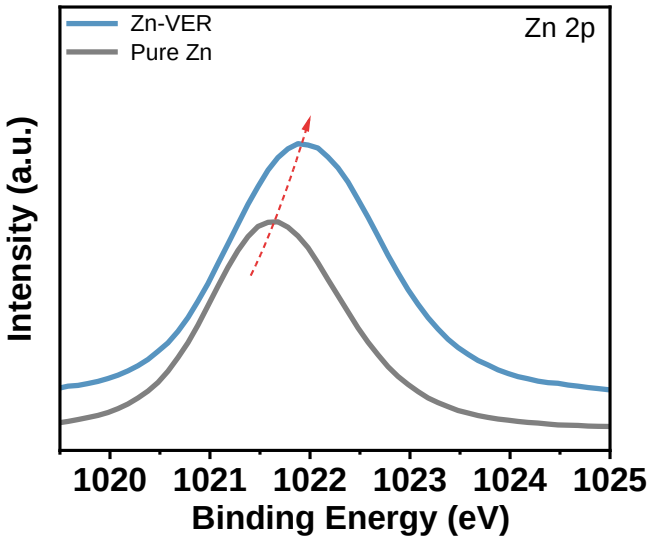


**Fig. S3** Comparison of the high-resolution XPS spectra of Zn 2p between pure Zn sheet and the Zn sheet after soaked in 0.3 g $L^{-1}$ veratraldehyde solution

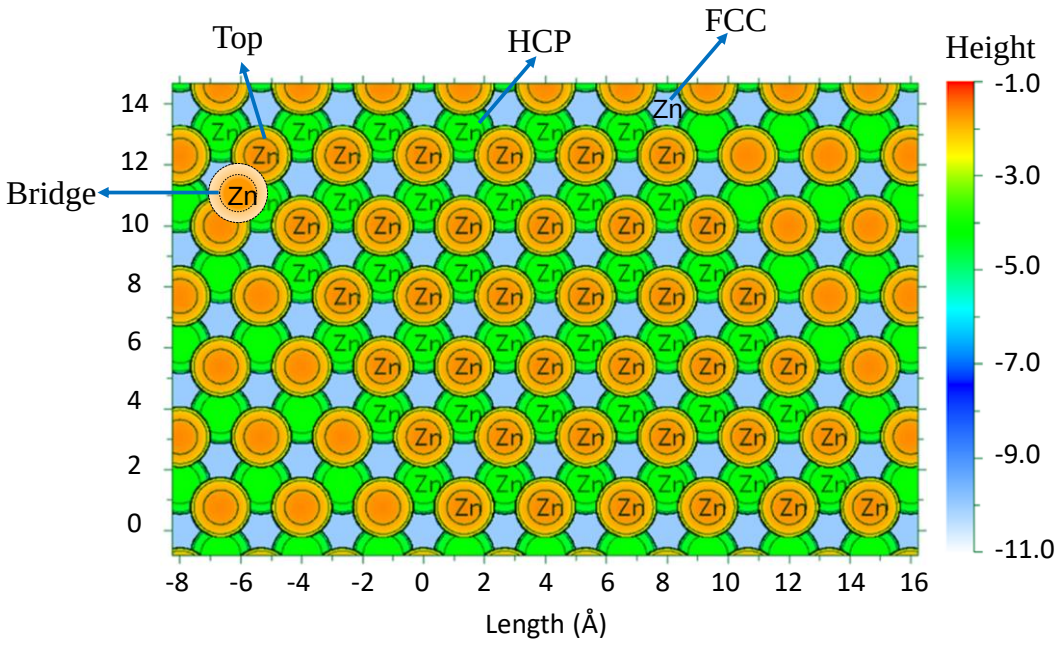


**Fig. S4** Top view of the Zn slab with possible absorbed sites

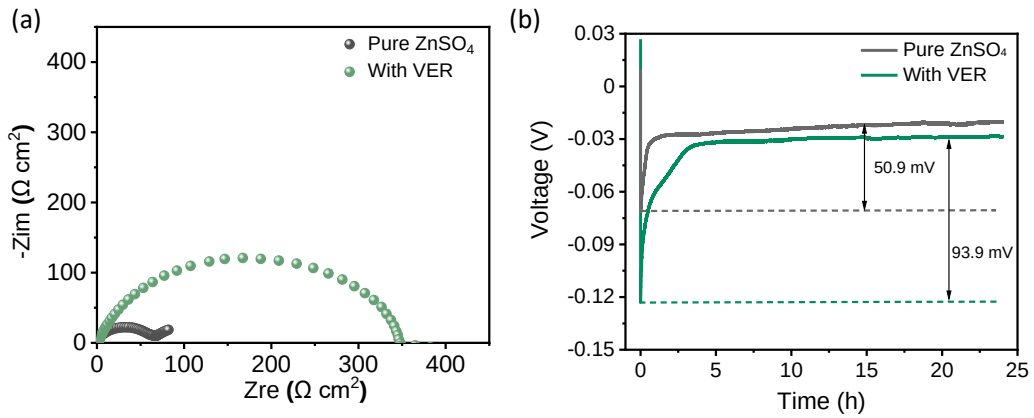


**Fig. S5** (**a**) EIS and (**b**) nucleation overpotential comparison of Zn-Zn symmetric cells under electrolyte systems with and without veratraldehyde additive

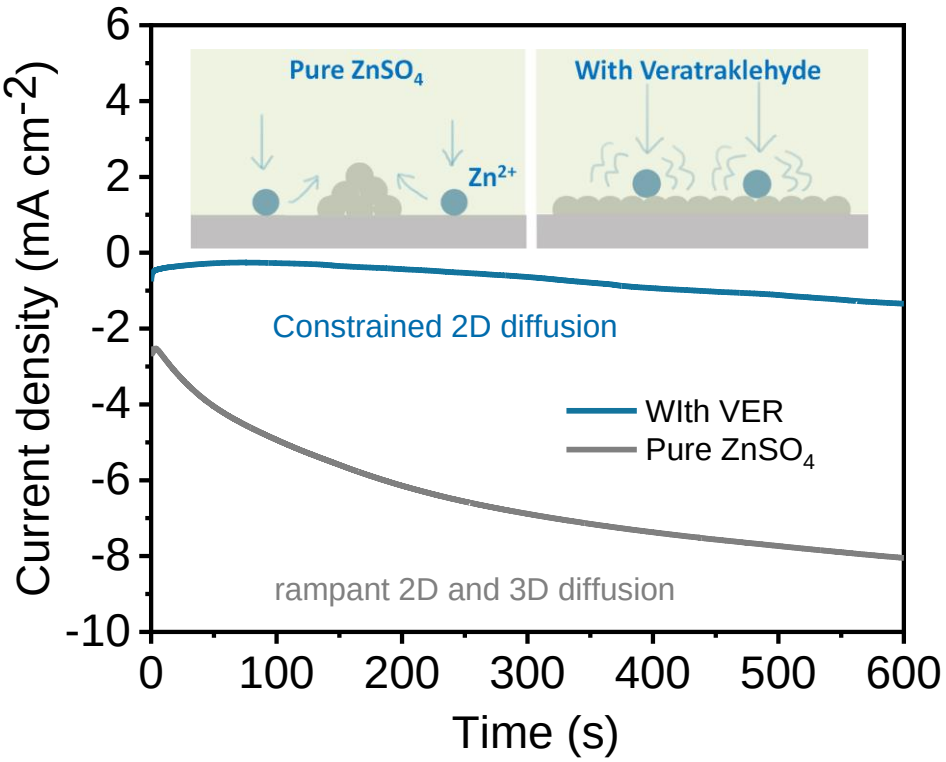


**Fig. S6** Chronoamperometry curves indicating $Zn^{2+}$ diffusion process of Zn electrode under different electrolyte system

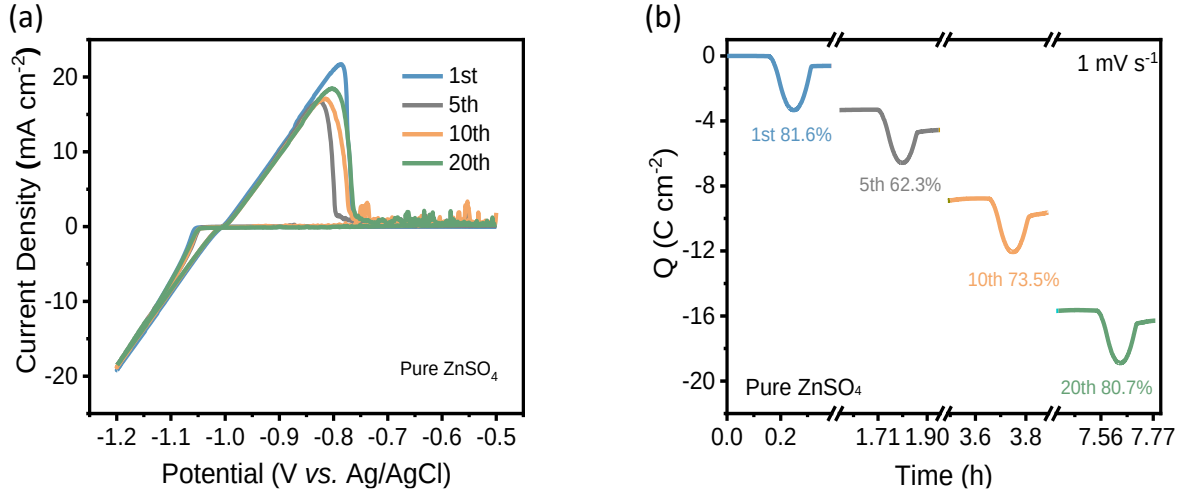


**Fig. S7** (**a**) CV curves of Zn plating/stripping at a scan rate of 1 mV $s^{-1}$ in the pure $ZnSO_4$ electrolyte and (**b**) corresponding chronocoulometry curves based on above CV curves

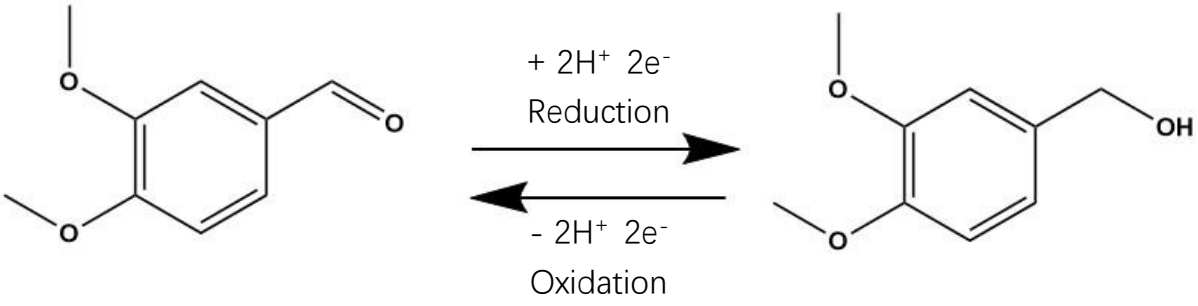


**Fig. S8** Reaction formula of reversible redox process between the veratraldehyde and veratryl alcohol molecules

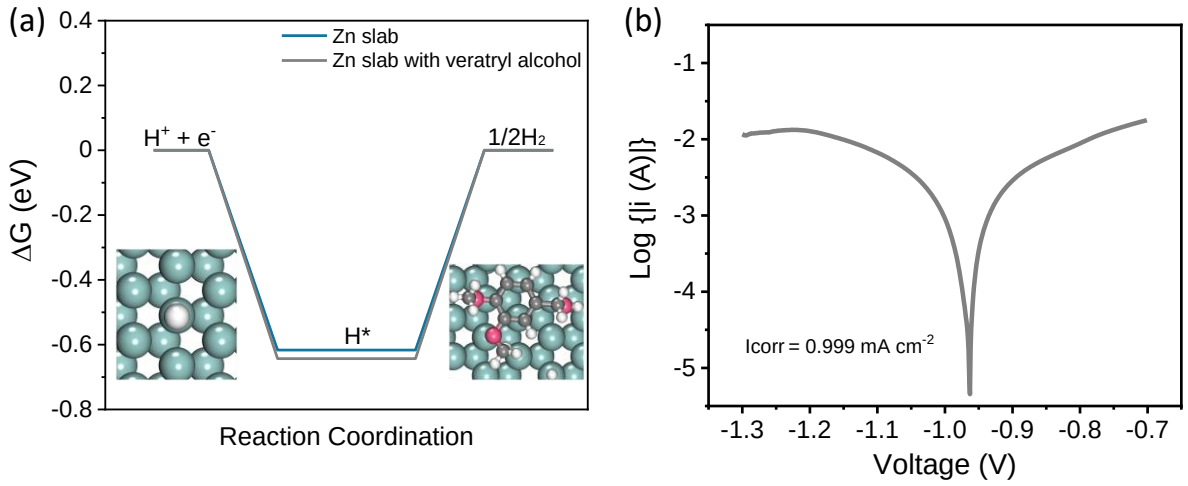


**Fig. S9** (**a**) The HER diagrams of pure Zn slab and Zn slab with absorbed veratryl alcohol; (**b**) Tafel plot representing the corrosion behavior under ZnSO4-veratryl alcohol electrolyte

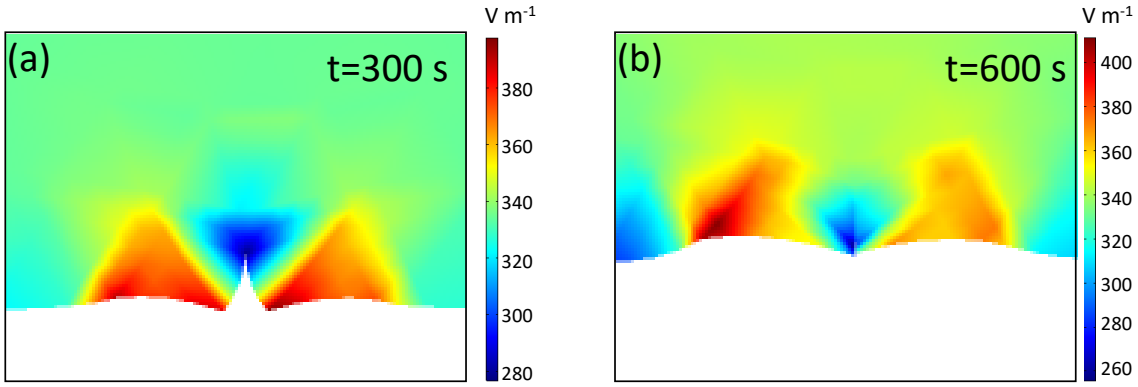


**Fig. S10** Models of electric field intensity distribution under (**a**)-(**b**) $ZnSO_4$-veratraldehyde electrolytes at different reaction time

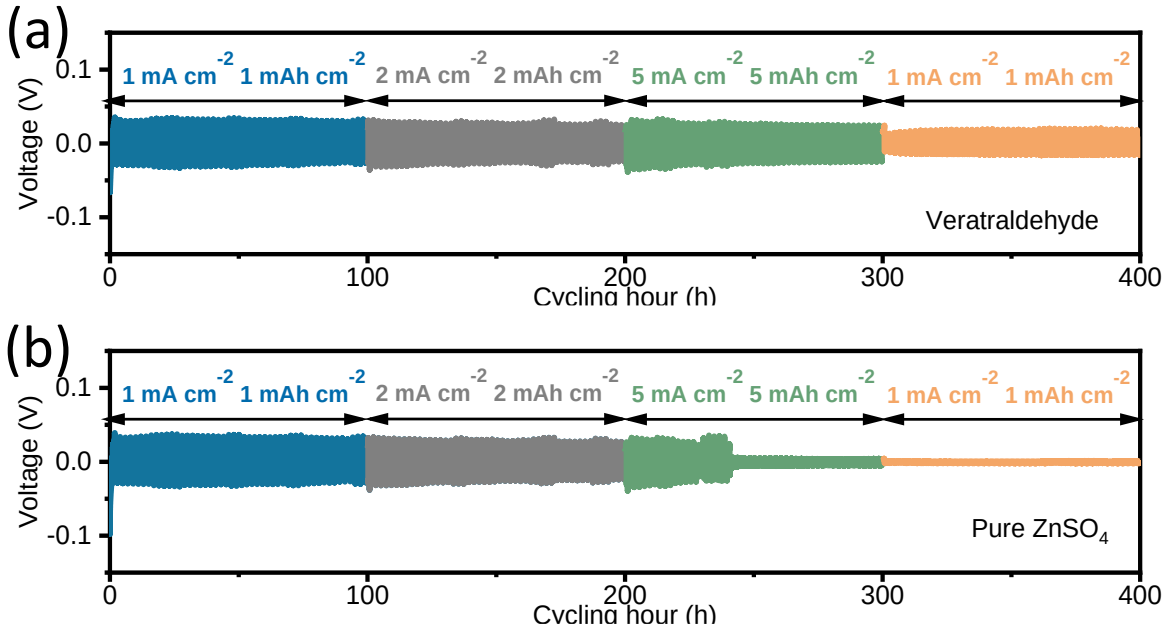


**Fig. S11** Rate cycling performance comparison of Zn-Zn symmetric cells under different current densities and areal capacities of 1 mA $cm^{-2}$, 1 mAh $cm^{-2}$; 2 mA $cm^{-2}$, 2 mAh $cm^{-2}$ and 5 mA $cm^{-2}$, 5 mAh $cm^{-2}$ in (**a**) $ZnSO_4$-veratraldehyde and (**b**) pure $ZnSO_4$ electrolytes

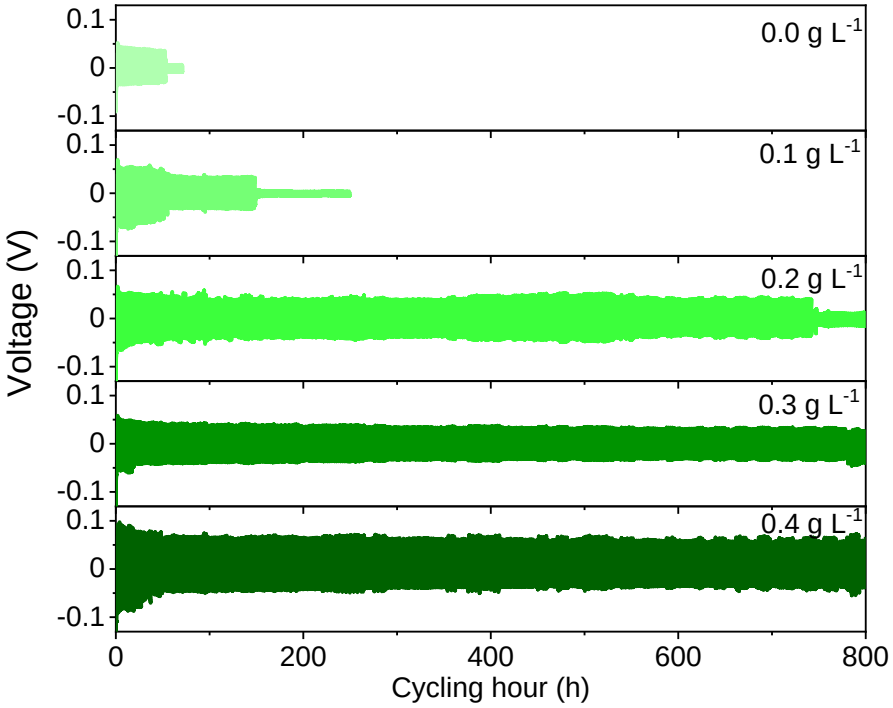


**Fig. S12** Long-term cycling performance comparison of Zn-Zn symmetric cells under current densities and areal capacities of 5 mA $cm^{-2}$, 5 mAh $cm^{-2}$ in $ZnSO_4$ electrolytes with different veratraldehyde concentration

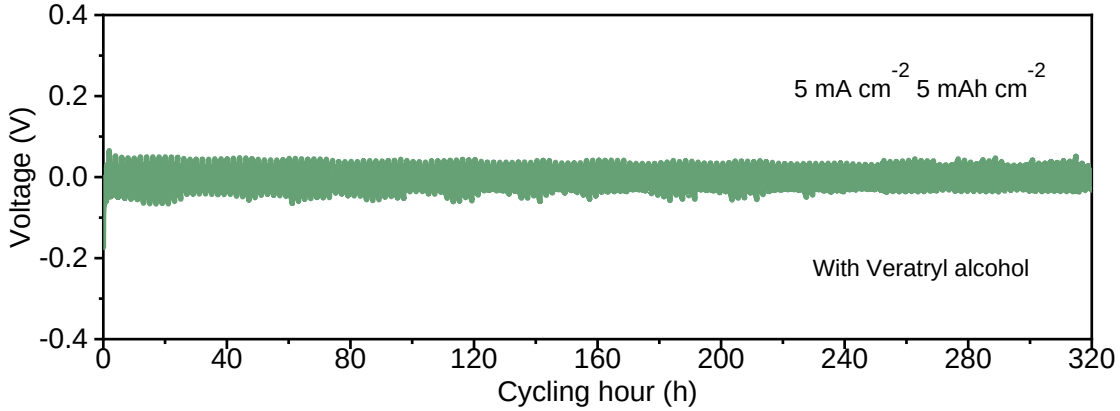


**Fig. S13** Long-term cycling performance comparison of Zn-Zn symmetric cells under current densities and areal capacities of 5 mA $cm^{-2}$, 5 mAh $cm^{-2}$ in $ZnSO_4$ electrolytes with alcohol additive

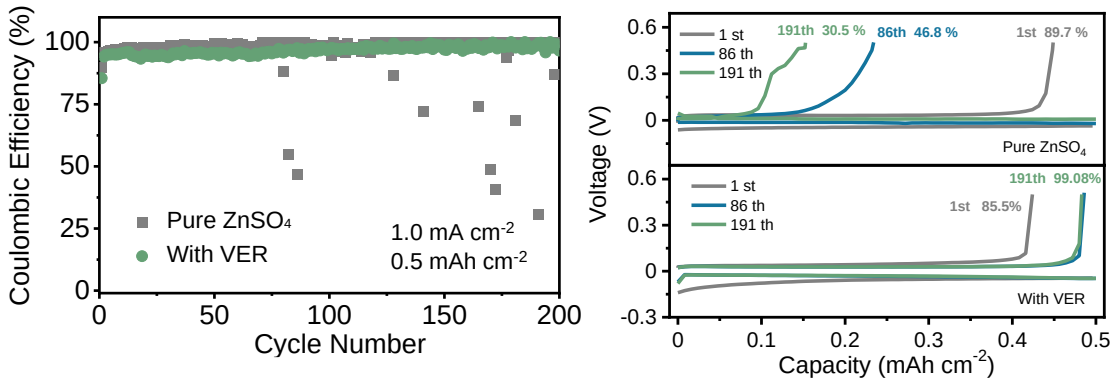


**Fig. S14** Coulombic efficiency (CE) measurements of Zn//Ti cells and corresponding voltage profiles at various cycles under pure $ZnSO_4$ and $ZnSO_4$-veratraldehyde electrolytes

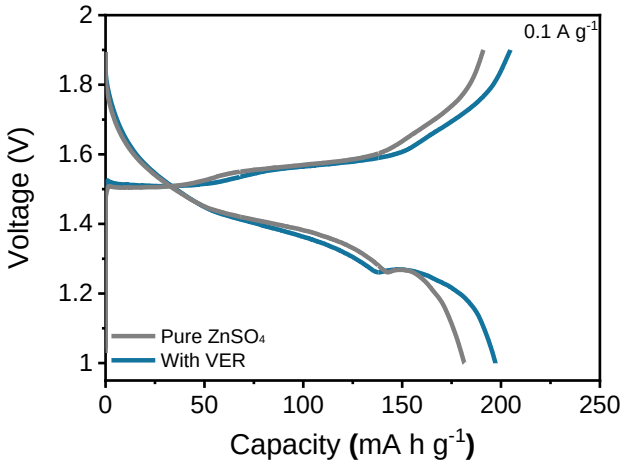


**Fig. S15** GCD curves at a current density of 0.1 A $g^{-1}$ in different electrolytes

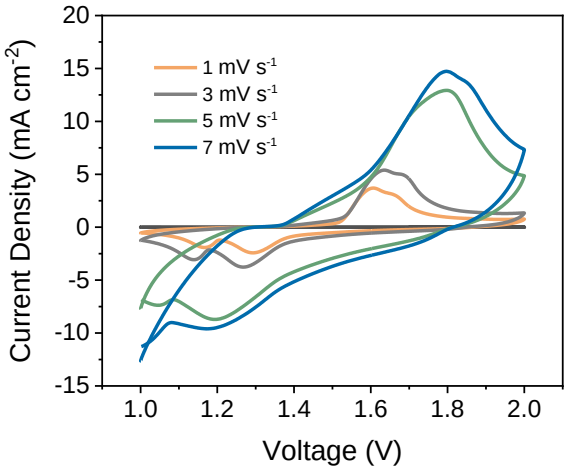


**Fig. S16** CV curves of Zn-$MnO_2$ batteries under different scan rates ranging from 1 mV $s^{-1}$ to 7 mV $s^{-1}$

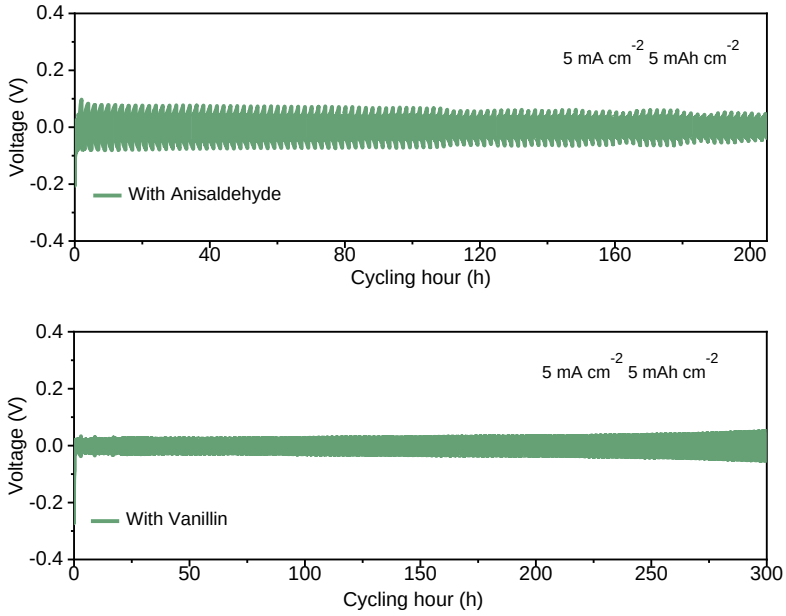


**Fig. S17** Long-term cycling performance comparison of Zn-Zn symmetric cells under current densities and areal capacities of 5 mA $cm^{-2}$, 5 mAh $cm^{-2}$ in $ZnSO_4$ electrolytes with anisaldehyde and vanillin additives